The large *N* behaviour of the Lipkin model and exceptional points

2005 J. Phys. A: Math. Gen. 38 1843

(http://iopscience.iop.org/0305-4470/38/9/002)

INSTITUTE OF PHYSICS PUBLISHING JOURNAL OF PHYSICS A: MATHEMATICAL AND GENERAL

J. Phys. A: Math. Gen. **38** (2005) 1843–1851 doi:10.1088/0305-4470/38/9/002

The large N behaviour of the Lipkin model and exceptional points

W D Heiss, F G Scholtz and H B Geyer

Institute of Theoretical Physics and Department of Physics, University of Stellenbosch, 7602 Matieland, South Africa

Received 22 September 2004, in final form 13 January 2005
Published 16 February 2005
Online at stacks.iop.org/JPhysA/38/1843

Abstract

The ubiquitous Lipkin model is investigated for an interaction parameter beyond the traditional critical point. It is argued that a phase transition occurs higher up in the spectrum for such larger interaction, where, using appropriate scaling of the energies, the position of the phase transition becomes independent of the particle number. The phase transition is related to near singularities in the complex interaction plane, the exceptional points. Consideration of finite temperature yields the well-known physical features associated with phase transitions.

PACS numbers: 05.30.−d, 02.30.−f, 71.10.Li

1. Introduction

One of the most intriguing problems in many-body physics concerns phase transitions (see, e.g., [1]). While from a classical viewpoint a phase transition is usually associated with a system of infinitely many particles, in quantum systems finite systems are more often investigated. The typical quantum phase transition is encountered at a particular value of a suitable parameter being usually an interaction strength and not the temperature; in fact, zero temperature transitions fall exclusively into the realms of quantum physics.

Typical examples are found in nuclear physics [2] where one speaks about transitions from a normal to a superconducting nucleus, from a spherical to a deformed nucleus, shape transitions of deformed nuclei, onset of tilted rotations, to mention just a few. For an infinite system the quantum analogue of the classical liquid–gas transition is still awaiting experimental confirmation in nuclear or quark matter. Phase transitions have also received considerable attention within the interacting boson model (IBM) [3] (see also [4] for recent developments and further references). Spin systems are naturally favoured subjects for the study of quantum phase transitions [1], and here the thermodynamic limit, that is the limit $N \to \infty$, $V \to \infty$ at constant density (with N being the particle number) is, for certain models, well understood.

0305-4470/05/091843+09$30.00

Once the spectrum is known, consideration of finite temperatures is then straightforward employing the standard procedures of statistical physics.

In many cases, however, the thermodynamic limit is problematic, even in models that have been thoroughly investigated owing to their attractive features for finite N. One case in point is the popular Lipkin model [5] that has served as a prime example for a quantum phase transition including spontaneous symmetry breaking [6]. We re-visit the model with particular emphasis upon the large N behaviour. Using methods developed recently [7] allowing calculation of the spectrum for virtually unlimited (yet finite) values of N, we scrutinise the properties of the model for a larger range of the interaction strength than was done traditionally where the emphasis was focused upon the phase transition affecting only the low-lying states. Particular emphasis is put on the singularities affecting the phase transition [8], singularities also affecting the partition function [9, 10]. In this way, a deeper understanding of the properties of the spectrum is achieved. It is hoped that the study, even though it concentrates on the Lipkin model, provides insight of a more universal nature.

In the following section, we rehash the basics of the model and discuss the essential properties for large values of N. Next the singularities, the exceptional points (EP) of the model are introduced and their patterns emerging for increasing N investigated. The connection between the findings of section 2 and the EPs is thoroughly discussed. A section about finite temperature underlines the physical relevance of the present study. The last section summarizes the essential findings and discusses problems still left open.

2. The Lipkin model for large N

The Lipkin model in its original form [5] considers interacting fermions occupying two Ω-fold degenerate levels. Its major appeal lies in the easy solubility [6] and the demonstration of a quantum phase transition including spontaneous symmetry breaking. The essential form is given in terms of $2j+1 = (N+1)$-dimensional representations of the $SU(2)$ operators J_z and $J_\pm = J_x \pm \mathrm{i}J_y$, N being the number of particles. It reads in dimensionless form

$$H(\lambda) = J_z + \frac{\lambda}{2N}\left(J_+^2 + J_-^2\right). \tag{1}$$

Here the interaction is scaled by N to ensure that H is extensive, the operators J_+^2 and J_-^2 effectively scale as N^2. In this form the model has a phase transition just beyond $\lambda = 1$, the larger N the closer the transition point at $\lambda = 1$. This has been discussed under various points of view in the literature, see, e.g., [6, 11]. Without scaling the interaction, the phase transition shifts close to $\lambda = 0$ and is difficult to identify, especially for relatively small particle number N.

The Hamiltonian allows reduction into two spaces: m integer and m half-integer, with m the eigenvalues of J_z; it corresponds to N even and odd, respectively, and is denoted as parity. For $\lambda \gtrsim 0$ the N-even and N-odd levels are obviously separated and remain so for all $\lambda < 1$ while the levels become degenerate (up to terms $\sim O(1/N)$) for $\lambda > 1$. The phase at $\lambda < 1$ is called the normal phase while the symmetry (parity) breaking phase at $\lambda > 1$ is called the deformed phase. Recent investigations [6] apply non-perturbative flow equations. This method allows to push the value of N to basically arbitrarily high yet finite values to obtain the spectrum.

A suitable order parameter is $\Lambda = 1 + J_z/j$. Its ground-state expectation value vanishes in the normal phase, but not in the deformed phase. The spectrum is conveniently arranged in ascending order: $E_0 \leqslant E_1 \leqslant \cdots E_N$. As the spectrum is symmetric around $E_{N/2} = 0$ [7], we can restrict ourselves to the set $E_0 \leqslant E_1 \leqslant \cdots E_{N/2}$. Instead of the discrete label

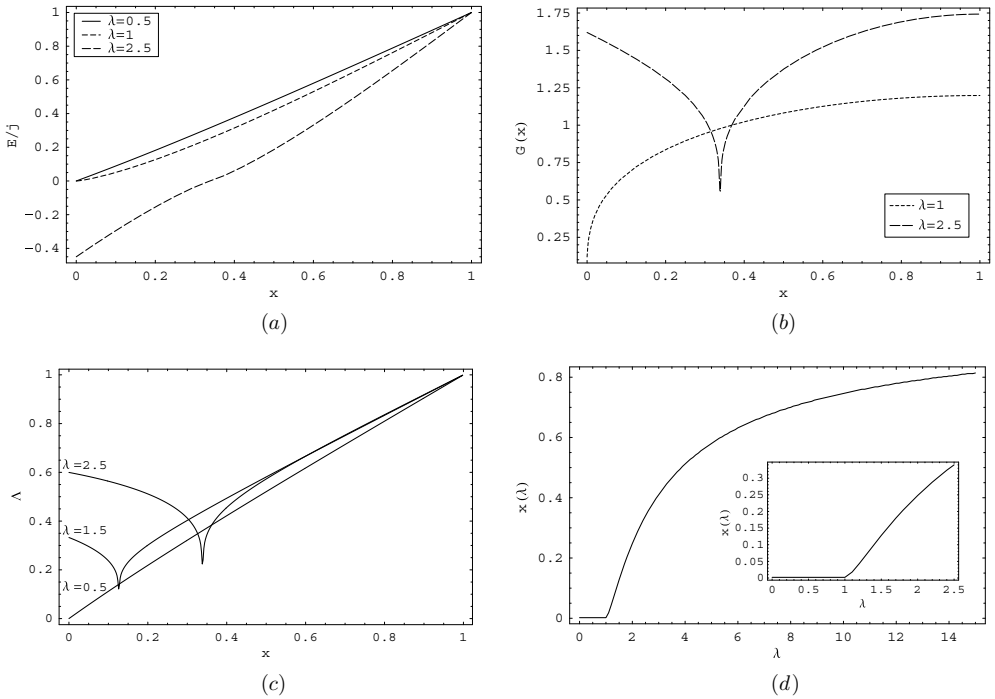

Figure 1. (*a*) Spectra normalized at $x = 1$ as a function of x for $N = 10^5$ and $\lambda = 0.5$, 1 and 2.5. (*b*) Level spacing $G(x) = \mathrm{d}E(x)/\mathrm{d}x$ for $\lambda = 1$ and 2.5. Only values for $\lambda \geqslant 1$ are shown as the level spacing vanishes only in this case. (*c*) Order parameter as a function of x for $\lambda = 0.5$, 1.5 and 2.5 and (*d*) phase diagram in the x–λ plane. Above the curve the system is in the normal phase and below in the deformed phase.

$k = 0, 1, \ldots, N/2$ we introduce, for large N, the continuous ratio $x = k/j \in [0, 1]$ indicating the position in the spectrum. Below we label the eigenvalues as $E(x)$ with the understanding that $E(0)$ and $E(1)$ denote the ground state and $E_{N/2}$, respectively.

In figure 1(*a*), the spectrum is illustrated for a few values of λ and $N = 10^5$. Note that, on this scale, the difference between N even and odd is invisible. Also, the spectrum appears as a continuous line since the individual states cannot be resolved when plotted against x. By scaling the energy with $1/j$, we ensure that for larger values of N we basically find the same drawings. The figure displays levels only up to $N/2$ ($x = 1$) owing to the symmetry of the spectrum around $N/2$.

Figure 1(*b*), shows the derivative $G(x) = \mathrm{d}E(x)/\mathrm{d}x$ being the level distance. The essential point is that the minimum occurs always at the same value x_0, independent of N, once a fixed value $\lambda = \lambda_{x_0} > 1$ is chosen. This pronounced minimum is characteristic for the phase transition and occurs only for $\lambda > 1$. As is discussed below, the level distance tends towards zero at $\lambda = \lambda_{x_0} > 1$ in the large N limit. However, for finite N, the transition remains soft and thus appears as a second-order transition. In figure 1(*c*) the order parameter $\Lambda = 1 + \langle J_z \rangle / j$ is shown as a function of x. Since the expectation value of the order parameter is evaluated with respect to states ranging from the ground state ($x = 0$) up to the state in the middle of the spectrum ($x = 1$), it does not vanish even in the normal phase, i.e., for $\lambda < 1$; it does vanish in the ground state for these λ-values. For all values of λ the normal phase is characterized by Λ being a linear function of x as then the eigenstates of the Hamiltonian are in fact approximate

eigenstates of J_z. Thus, as we move up in the spectrum, Λ will scale linearly with x beyond the minimum signalling for $\lambda > 1$ the transition from the deformed to the normal phase. This minimum is likewise independent of N, its position coincides with that in figure 1(b). The diagram demonstrates that, for given $\lambda = \lambda_{x_0}$, the transition from the deformed state (all levels below $E(x_0)$) to the normal state (all levels above $E(x_0)$) occurs at energies around $E(x_0)$. The corresponding phase diagram showing the x–λ dependence is illustrated in figure 1(d). It represents the value of x where for a given λ_x the minimum in the level spacing and in the order parameter occurs thus specifying the position of the phase transition. The actual values of the minimum distances between levels around $E(x_0)$—and this is the only change in figure 1(b) and (c) when N is increased—tend towards zero with increasing N.

This property of the model did not, to the best of our knowledge, attract any attention in the literature. Traditionally, the interest was focused upon the low-lying levels and for these the phase transition occurs at $\lambda \gtrsim 1$ for large N. The fact that higher up in the spectrum the levels remain unperturbed for $\lambda \simeq 1$, and that the change from the normal to the deformed state happens higher up in the spectrum for $\lambda > 1$ appears to be of interest for an understanding of the thermodynamic limit ($N \to \infty$).

This limit is well understood for the normal phase, i.e., for $0 \leqslant \lambda < 1$ where the Holstein–Primakoff transformation [12] to boson operators $(b, b^\dagger)$ reduces the Hamiltonian (1) to a quadratic boson Hamiltonian which may be diagonalized with the standard Bogoliubov transformation, yielding readily a harmonic spectrum $E_k = k\sqrt{1-\lambda^2}, k = 1, 2, \ldots$. Note that this result implies that the whole spectrum collapses to zero at $\lambda = 1$. However, as the Bogoliubov transformation becomes singular at this point, this would be a naive conclusion. In fact, the boson Hamiltonian reduces at $\lambda = 1$ (up to a factor) to $(b + b^\dagger)^2 \sim x^2$ having a continuous spectrum. As it is clear from the discussion above and from the following section, the limit is much more subtle for $\lambda \geqslant 1$, if it exists. We mention that a mean field approach [13, 14] does yield for $\lambda > 1$, the excitation spectrum $E_k = k\sqrt{2(\lambda^2 - 1)}, k = 1, 2, \ldots$, but as a mean field approach it focuses upon the ground-state properties and cannot reproduce the rich complexity of the model. Also the more sophisticated time-dependent Hartree–Fock calculations [15] can neither reproduce the fluctuations around the transition point nor the transition higher up in the spectrum.

In the following section, we view the properties of the model from a different angle by concentrating upon the singularities of the spectrum associated with a phase transition [8, 9]. These singularities are the exceptional points of the Hamilton operator [16]. They also appear to play a pivotal role not only in phase transitions but also in specific approximation schemes [17].

3. Exceptional points

To facilitate technicalities, we slightly modify the original model by using instead

$$H(\lambda) = H_0 + \lambda H_1 \qquad H_0 = k\delta_{k,k'}$$
$$H_1 = \frac{N}{8}\left(1 - \left(1 - \frac{2k}{N}\right)^2\right)\delta_{k,k'-1} + \text{h.c.} \tag{2}$$

with $k, k' = 1, \ldots, N$. This irreducible form (as opposed to the form (1) where the even and odd N spaces decouple) reproduces the model perfectly well [18]. It has the advantage that the roots of high-order polynomials occurring in the calculation of EPs can be calculated exactly using *Mathematica*. The EPs in the λ-plane are obtained from the simultaneous roots of the

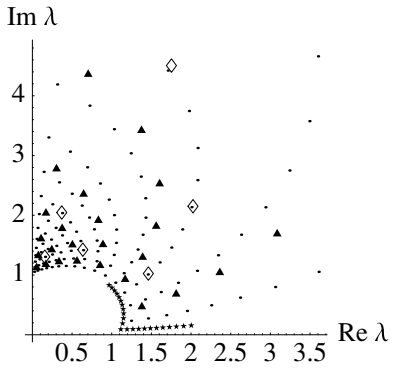

Figure 2. Exceptional points in the λ-plane for $N = 8$ (diamonds), $N = 16$ (triangles) and $N = 32$ (dots). The first twelve starting points of the arcs and of the innermost arc running from the real to the imaginary axis are indicated by asterisks for $N = 96$.

two polynomials [20]

$$P(E) = \det(E - H(\lambda)) \qquad P'(E) = \frac{\mathrm{d}}{\mathrm{d}E}\det(E - H(\lambda)). \tag{3}$$

Eliminating the variable E yields the resultant being a polynomial in λ of order $N(N-1)$. In fact, the resultant is a polynomial $Q(z)$ of order $N(N-1)/2$ in $z = \lambda^2$. With the form of the Hamiltonian given in equation (2), $Q(z)$ factorizes. For N even, we have

$$Q(z) = S(z)(T(z))^2 \qquad S(z) = \prod_{k=1}^{N/2}\left(z + \frac{N^2}{(N-(2k-1))^2}\right) \tag{4}$$

with $T(z)$ a polynomial of order $((N-1)^2 - 1)/4$. For N odd there is a similar factorization but the roots of $S(z)$ are less simple. From the roots of $S(\lambda^2)$, we obtain EPs on the imaginary λ-axis at

$$\lambda_k = \pm \mathrm{i}\frac{N}{N-(2k-1)} \qquad k = 1, \ldots, \frac{N}{2} \tag{5}$$

which are of lesser interest as we focus our attention on EPs close to the real axis. They are obtained from the roots of $T(\lambda^2)$. We note that the symmetry of the model generates EPs in the complex plane in such a way that for each λ there are the mirror points $-\lambda$, λ^*, $-\lambda^*$.

In figure 2, these roots are illustrated in the first quadrant of the λ-plane for $N = 32, 16, 8$ by solid dots, triangles and diamonds, respectively. For clarity, we restrict ourselves to small numbers of N, also a few more points occurring outside the range shown are not displayed. The qualitative pattern emerging for increasing N is obvious: (i) there is no EP within the unit circle; (ii) outside $|\lambda| = 1$ there are geometric patterns forming in each quadrant: 'circular-like arcs' around the origin where the innermost arc contains $N/2$ EPs—including the one at $\mathrm{i}N/(N-1)$ (not shown), the next arc contains $(N/2-1)$ EPs—including the one at $\mathrm{i}N/(N-3)$ and so forth; (iii) with increasing N the starting points near to the real axis of the arcs move closer to the real axis, in fact, they converge to the point $\lambda = 1$; (iv) for a fixed value of $\lambda_x > 1$ there is a fixed fraction of $N/2$, say $xN/2$, $x \in [0, 1]$, of starting points with their real parts between $\lambda = 1$ and $\lambda = \lambda_x$: the example of the drawing has $1/4 \times N/2 = N/8$ such points on the left of $\lambda_{1/4} \approx 2.01$; we have inserted into figure 2 the first twelve of such starting points and the first twelve of the innermost arc for $N = 96$ by asterisks.

Inspection of the levels coalescing at these points reveals that at the point nearest to $\lambda = 1$, E_1 and E_2 coalesce. At the point next to it to the right, E_2 and E_3 coalesce, next to

the right E_3 and E_4 coalesce and so forth. We mention that for the row of points just above the row of the starting points we now have E_2 and E_3 coalescing at the first, E_3 and E_4 at the next point to the right and so forth. As the levels of the model are perfectly symmetric around the level $E_{N/2}$, the point $\lambda_{k,k+1}$ where E_k and E_{k+1} coalesce coincides with the point where E_{N-k+1} and E_{N-k} coalesce, but it lies of course in a different Riemann sheet. For instance, at the point nearest to $\lambda = 1$, E_1 and E_2 coalesce on the bottom sheet and E_{N-1} and E_N coalesce at the same point on the top sheet. We concentrate our interest upon the lower half of the spectrum and the EPs near to the real λ-axis.

From these insights the discussion of the previous section appears now much elucidated. Recall that an EP positioned near to the real axis is associated with level repulsion: the nearer the EP to the real axis, the smaller the gap between the two participating levels for real λ. In the model considered, there is for large N a dense set of EPs close to the real axis for $\lambda > 1$. For a particular point λ_{x_0}, the levels around $E(x_0)$ approach each other closest, it is in this range of levels where the phase transition happens. Energies much below $E(x_0)$, in particular the corresponding eigenstates, have all the properties of the deformed phase of the interacting system while the eigenstates of the energy range above $E(x_0)$ are unperturbed. The phase transition traditionally associated with $\lambda = 1$ refers to the energy range adjacent to the ground state, here we associate it with $x = 0$. Above we found $\lambda \approx 2$ associated with $x = 1/4$. The symmetry of the levels around $N/2$ yields the limit $\lambda = \infty$ for $x = 1$. The phase diagram depicted in figure 1(*d*) illustrates $x(\lambda)$.

The absence of EPs for $\lambda < 1$ has the effect that all eigenstates are localized and well described in the unperturbed basis, i.e., in this basis just a few states contribute to each eigenstate. Only when the critical point $\lambda = 1$ is approached do the low-lying eigenstates become strongly mixed owing to the proximity of EPs associated with coalescences of the low-lying states. From the discussion above, it is clear that an appreciable portion of low-lying states becomes involved, the more so the larger N. Yet the states higher up are still basically unperturbed as they do not coalesce for λ-values with $\mathrm{Re}\,\lambda$ equal to unity. Increasing λ, however, further beyond unity the low-lying states are then well described and localized in the deformed basis as, for λ sufficiently distant from unity, there are no nearby EPs that could mix them. It is now the states higher up that are extended (i.e. *not* localized) as they are affected by closely lying EPs: from the inset in figure 1(*d*) we read off that, for instance, at $\lambda \approx 1.19$ the states around $E_{N/50}\,(x = 1/25)$ are coalescing near to the real λ-axis and therefore strongly mixed. And this trend continues according to figure 1(*d*).

From figure 2 and the discussion relating to it, it becomes clear that the average distance between the real parts of two adjacent EPs near to the real axis is $\sim 1/N$. In fact, the number of EPs nearest to the real axis increases proportionally to N; in figure 2, between $\lambda = 1$ and ≈ 2, we discern one, two, four and twelve EPs for $N = 8, 16, 32$ and 96, respectively. Note that the same law holds on the imaginary axis as we conclude from equation (5). For the real parts of EPs near to the real axis, this implies a rate of approach of the critical point $\lambda = 1$ to behave $\sim 1/\log(N)$ (apart from possible logarithmic terms of higher order). The rate of approach towards the real axis, i.e., the vanishing of the respective imaginary parts appears to be at a faster rate. Numerical evidence seems to indicate a power law at $\lambda = 1$. This is in line with the behaviour of the closest distance—showing at $\lambda = 1$ a $N^{-1/3}$ behaviour [19]—between avoiding levels. Exploiting proportionality of level distance and imaginary part of the EP [20], we conclude the same $N^{-1/3}$ behaviour for the imaginary parts of the EPs zooming in at $\lambda = 1$. The level distance tends towards zero around $E(x_0)$ for any specific $\lambda = \lambda_{x_0} > 1$, yet seemingly at a lower rate. For $\lambda_{x_0} \gg 1$, it may not even be a power law but $\sim 1/\log(N)$ (note: these asymptotic behaviours are valid without the traditional scaling

factor $1/j$ usually applied as in figure 1(a) to accommodate the unboundedness from below of the Hamiltonians (1) and (2) in the limit $N \to \infty$).

A few comments are in order relating to the thermodynamic limit. Naively, one might expect each point on the real line to be an accumulation point of EPs. While it is known that an operator cannot be diagonalized at an isolated EP [21], an accumulation point can also have this property [22]. This would contradict the naive expectation that the Hamiltonian (2) remains self-adjoint in the thermodynamic limit and should therefore be diagonalizable. That such limit (if it exists) is bearing special features, follows from the discussion of this and the previous section: for $\lambda = \lambda_x$ the distance between levels around $E(x)$ vanishes for $N \to \infty$. Whether it signals the onset of a continuum or an infinite degeneracy is not clear. We leave these mathematical issues at this point as they do not seem to have obvious physical ramifications.

4. Finite temperature

The Lipkin Model has been the focus of a number of finite temperature calculations [23, 24, 14], mostly to study and compare various approximation schemes of the mean-field type and the incorporation of $1/N$ (or $1/\sqrt{N}$) effects [14]. To the extent that phase transitions at finite temperature are investigated, it is concluded in these studies that any firm indications of discontinuities are artefacts of approximation schemes that are not supported by exact calculations. Our findings below contrast with this as we are able to avoid the limitations of the many-body techniques pointed out in [14, 23, 24], and we can also explore much larger values of the particle number N. Also it appears doubtful as to whether restriction to an expansion in terms of powers of $1/\sqrt{N}$ can do justice to the complexity of the model in view of the logarithmic behaviour becoming dominant for $\lambda > 1$ and the $1/N^{1/3}$ behaviour at $\lambda = 1$.

We note that there is a close relationship between EPs and the zeros of the partition function [9, 10]. However, in [9] the complex temperature plane is discussed while we consider the complex plane of the interaction strength.

In our analysis knowledge of the spectrum is obtained through the flow equation analysis [7], yielding the canonical partition function and thus the heat capacity in the standard way. From the properties of the spectrum one would expect the system to behave for $\lambda < 1$ essentially as a harmonic oscillator: for large values of kT the heat capacity approaches the constant value 1 in units of k (here we measure kT in dimensionless units in line with the dimensionless Hamiltonian (1)). For the values of $\lambda > 1$, one expects the phase transition to occur higher up in the spectrum and to exhibit a peak in the heat capacity at temperatures kT being of the order of the energy where the phase transition occurs. Thus, this peak is expected to move to higher temperatures with increasing λ since, as is clear from figures 1(b)–(d), the phase transitions moves up in the spectrum with increasing λ. In figure 3(a), the heat capacity is illustrated as a function of the dimensionless kT. The expected features can all be clearly seen from this graph. The rather broad peaks in the heat capacity originate from the finite size of the system ($N = 1000$ in figure 3(a)); also the values of $\lambda > 1$ shown in figure 3(a) relate to the phase transition at comparatively high energies, where the temperature is appreciably larger than the level spacing. We note that the heat capacity cannot vanish at large temperature in the thermodynamic limit; the results of figure 3 in [24] are explained by a too small value of N leading to a quick saturation of possible heat absorption.

The interpretation of a phase transition at higher energy is further supported by figure 3(b) illustrating the ensemble average of the order parameter $\langle \Lambda \rangle$ as a function of kT. Only $\lambda > 1$ is displayed, as the order parameter is structureless for smaller values, where it behaves linearly

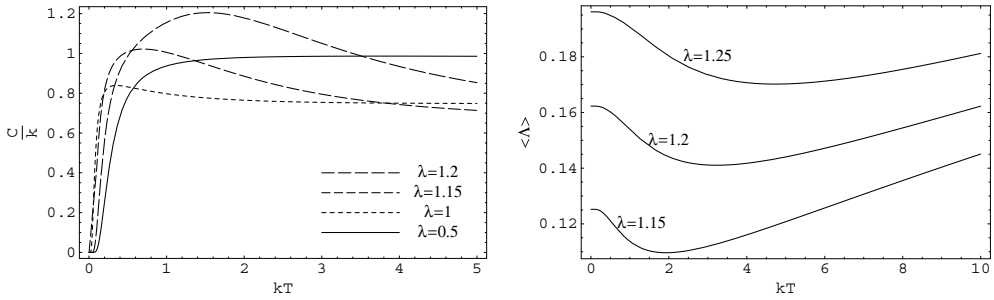

Figure 3. (*a*) Heat capacity of the Lipkin model in units of k as a function of the dimensionless kT. (*b*) Order parameter as a function of kT.

with kT. One clearly observes a rapid decrease in the order parameter at a temperature where kT is of the order of the energy where the levels have their minimum distance, signalling the transitions from the deformed to the normal phase. Above this point it increases linearly with kT as is expected in the normal phase. Furthermore, this point moves up in temperature as the coupling constant is increased, consistent with our previous observations. Since the rate of convergence towards the thermodynamic limit is the weaker the larger the λ, the transitions appear rather soft in figure 3 as they are evaluated for finite N.

The model demonstrates that the avoided level crossings, associated with the accumulation of exceptional points higher up in the spectrum, manifest themselves as an observable effect at finite temperature. This result has an appealing physical meaning: for an interaction strength $\lambda \geqslant 1$, the system will be in the deformed phase at low but finite temperature; increasing the temperature induces the phase transition into the normal phase whereby the larger the interaction strength λ the higher the transition temperature.

5. Summary and outlook

Except for the figure illustrating the EPs the drawings remain basically unchanged when N is further increased. In this way, we have obtained the essential features of the behaviour of the model for large N. It turns out that the model has a much richer structure than what is discussed traditionally in the literature. In particular, the relation between the transition temperature and the interaction strength discussed in the previous section is an appealing aspect not treated in the literature. Note, that with suitable rescaling, that is by concentrating upon the upper half of the spectrum, the pattern discussed in the previous section can be turned around: in fact, denoting the state $E_{N/2}$ as the ground state and considering the range $E_{N/2} - E_N$, the normal state would prevail at low temperature and the deformed state would form at high temperature. Of course, we prefer the viewpoint adopted in this paper where the symmetry breaking state prevails at low temperature.

The connection with the singularities affecting the phase transition—irrespective of the high or low value of the transition temperature, i.e., the interaction strength—is well understood by considering the EPs of the model. From figure 2, it is clear how the pattern of the EPs is filling up the complex plane with increasing N. Yet, the limit attained is unclear. It can be expected that the points $\lambda = \pm 1$ and $\lambda = \pm \mathrm{i}$ are accumulation points, but whether and how the real axis $\lambda \geqslant 1$ (and $\lambda \leqslant -1$), the unit circle and the imaginary axis will be densely populated by EPs is not quite clear. This question has a bearing on the analytic connectedness

between the normal phase (inside the unit circle) and the deformed phase (outside $|\lambda| = 1$). Likewise, it has a bearing on the operator property of the deformed phase for $N \to \infty$. If the imaginary parts of the EPs along the real axis vanish in the limit, the operator is expected to be non-diagonalisable, its Jordan form would have the typical non-zero off-diagonals [21].

A question for future research is that of a random perturbation of the Lipkin model. A rather generic perturbation is expected to destroy the rigid geometrical pattern of the EPs by tossing them around [25]. Related to this is the question of the extended states: Will they become localized? It is important to note that this last question, being of particular physical interest, can be tackled for finite N and is not necessarily related to a mathematical limit. These and related problems, seemingly of a rather universal nature and interest, must be the subject of future research.

Acknowledgment

The authors are grateful to Hannes Kriel for preparation of some drawings. They acknowledge financial support by the South African National Research Foundation.

References

[1] Sachdev S 1999 *Quantum Phase Transitions* (Cambridge: Cambridge University Press)
[2] Bohr A and Mottelson B R 1975 *Nuclear Structure* (New York: Benjamin)
[3] Iachello F and Arima A 1987 *The Interacting Boson Model* (Cambridge: Cambridge University Press)
[4] Cejnar P, Heinze S and Jolie J 2003 *Phys. Rev.* C **68** 034326
[5] Lipkin H J, Meshkov N and Glick N 1965 *Nucl. Phys.* A **62** 188
Lipkin H J, Meshkov N and Glick N 1965 *Nucl. Phys.* A **62** 199
Lipkin H J, Meshkov N and Glick N 1965 *Nucl. Phys.* A **62** 211
[6] Ring P and Schuck P 1980 *The Nuclear Many Body Problem* (New York: Springer)
[7] Scholtz F G, Bartlett B H and Geyer H B 2004 *Phys. Rev. Lett.* **91** 80602
Kriel J N, Morozov A and Scholtz F G 2005 *J. Phys. A: Math. Gen.* **38** 205
[8] Yang C N and Lee T D 1952 *Phys. Rev.* **87** 410
[9] Borrmann P, Mülken O and Harting J 2000 *Phys. Rev. Lett.* **84** 3511
[10] Cejnar P, Heinze S and Dobes J *Preprint* nucl-th/0406060
[11] Pan Feng and Draayer J P 1999 *Phys. Lett.* B **451** 1
[12] Klein A and Marshalek E R 1991 *Rev. Mod. Phys.* **63** 375
[13] Gering M Z I and Heiss W D 1984 *Phys. Rev.* C **29** 1113
Heiss W D and Lemmer R H 1984 *Phys. Rev.* C **29** 2368
[14] Dzhioev A, Aouissat Z, Storozhenko A, Vdovin A and Wambach J 2004 *Phys. Rev.* C **69** 014318
[15] Kan K K, Lichtner P C, Dworzecka M and Griffin J J 1980 *Phys. Rev.* C **21** 1098
[16] Kato T 1966 *Perturbation Theory of Linear Operators* (Berlin: Springer)
[17] Khalil T and Richert J 2004 *J. Phys. A: Math. Gen.* **37** 4851
[18] Heiss W D 1988 *Z. Phys. A. At. Nucl.* **329** 133
[19] Dusuel S and Vidal J 2004 *Phys. Rev. Lett.* **93** 237204
[20] Heiss W D and Sannino A L 1990 *J. Phys. A: Math. Gen.* **23** 1167
[21] Heiss W D 2004 *J. Phys. A: Math. Gen.* **37** 2455
[22] Heiss W D, Müller M and Rotter I 1998 *Phys. Rev.* E **58** 2894
[23] Tsay Tzeng S Y, Ellis P J, Kuo T T S and Osnes E 1994 *Nucl. Phys.* A **580** 277
[24] Vdovin A I and Storozhenko A N 1999 *Eur. Phys. J.* A **5** 263
[25] Heiss W D and Sannino A L 1991 *Phys. Rev.* A **43** 4159